

1 Barrier-island migration dominates ecogeomorphic
2 feedbacks and drives salt marsh loss along the Virginia
3 Atlantic Coast, USA

4 **Charles D. Deaton^{1,*}, Christopher J. Hein², and Matthew L. Kirwan²**

5 ¹*Department of Geology, College of William and Mary, Williamsburg, Virginia 23185,*
6 *USA*

7 ²*Department of Physical Sciences, Virginia Institute of Marine Science, College of*
8 *William and Mary, Gloucester Point, Virginia 23062, USA*

9 *Current address: Institute of Marine Sciences, University of North Carolina at Chapel
10 Hill, Morehead City, North Carolina 28557, USA; E-mail: cddeaton@email.wm.edu.

11 **ABSTRACT**

12 Coupling between barrier islands and their associated backbarrier environments
13 (salt marsh, tidal flats) leads to complex ecogeomorphic feedbacks that are proposed to
14 control the response of barrier island systems to relative sea-level rise. This study tests
15 the applicability of these still theoretical concepts through investigation of the Virginia
16 barrier islands, which are located in a hotspot of accelerated sea-level rise. Using
17 historical maps and photographs from 1851 to 2010, we determine that rapid landward
18 island migration ($1\text{--}6 \text{ m yr}^{-1}$) is leading to backbarrier area reduction and large-scale salt
19 marsh loss (63 km^2 or 19%) at a rate of $0.45 \text{ km}^2 \text{ yr}^{-1}$. Landward barrier-island migration
20 far outpaces upland marsh migration and was responsible for 51% of marsh loss, with the
21 remainder due to backbarrier processes (e.g., edge erosion). In direct contrast to proposed
22 ecogeomorphic feedbacks linking barrier island and backbarrier environments, shoreline

23 retreat rates were not related to changes in backbarrier marsh, open-water areas, or tidal
24 prism. Rather, these results indicate that, for barrier island systems already undergoing
25 migration, the primary barrier-backbarrier coupling is the loss of marsh and tidal-flat area
26 because of barrier-island migration itself.

27 **INTRODUCTION**

28 Barrier islands are shore-parallel, elongated sand bodies that front 10% of the
29 world's coastlines (Stutz and Pilkey, 2011) and are backed by backbarrier marshes, tidal
30 flats, and lagoons, all of which serve to buffer coastal environments and human
31 development against relative sea-level rise (RSLR) and storms. Barrier islands and their
32 associated backbarrier environments (here called "barrier systems") support diverse
33 faunal communities and provide a wide range of ecosystem services and (Barbier et al.,
34 2011). Over historical time, *ca.* 70% of the world's barrier island shorelines – and 68% of
35 those along the U.S. New England and Mid-Atlantic coasts – are eroding (Bird, 1985;
36 Hapke et al., 2013). These changes primarily reflect forcings by RSLR, which shifts the
37 coastal areas affected by erosive forces (*i.e.*, waves and inundation) landward (Vellinga
38 and Leatherman, 1989), and changes in available sediment quality and quantity (Stutz
39 and Pilkey, 2011). At the same time, backbarrier salt marshes, which appear to have high
40 resilience to RSLR (Kirwan et al., 2016), are threatened by other anthropogenic stressors,
41 including eutrophication and sediment supply reduction (Kirwan and Megonigal, 2013).

42 Historically, marsh and barrier island evolution have been treated separately, but
43 recent work suggests that important couplings exist between their respective processes.
44 Modeling by Brenner et al. (2015) and Lorenzo-Trueba and Mariotti (2015) indicates that
45 backbarrier width and substrate are both important determinants in island migration and

46 response to RSLR, where islands with a sandier substrate and wider backbarrier
47 environment migrate landward more slowly. Similar work by Walters et al. (2014) and
48 Rodriguez et al. (2013) emphasize that overwash and aeolian processes are an important
49 sediment source for backbarrier marshes, allowing them to survive higher RSLR rates
50 than isolated marshes, and that the presence of island-adjacent backbarrier marshes slows
51 landward barrier island migration rates. Such ecogeomorphic feedbacks indicate that
52 these systems must be analyzed holistically to predict the response of barrier systems to
53 global change.

54 Barrier-backbarrier couplings have also been predicted to drive the rapid
55 degradation of barrier systems as a result of accelerated RSLR via “runaway
56 transgression” (FitzGerald et al., 2008). This conceptual model predicts that under rapid
57 RSLR rates, the backbarrier environment of mixed-energy barrier systems will undergo
58 submergence, converting marsh to open water and leading to an increase in tidal prism
59 (the volume of water transferred between the backbarrier and coastal ocean during a half
60 tidal cycle) and an attendant increase in the size of sandy ebb-tidal deltas. This process
61 would sequester sand otherwise available to adjacent islands, causing erosion-driven
62 narrowing to accelerate. Eventually, these processes would lead to island breaching and
63 rapid landward migration, destroying ecosystems and forfeiting the mainland protection
64 and storm resistance provided by barrier systems.

65 Linking the evolution of barrier island and backbarrier environments through
66 complex ecogeomorphic feedbacks represents an innovative framework for assessing the
67 stability of coastal barrier systems, yet remains largely untested with field observation.
68 Here, we test whether these concepts indeed govern the integrated evolution of barrier

69 systems by analyzing the 150-year geographic evolution of nine largely undeveloped,
70 mixed-energy barrier systems along the Eastern Shore of Virginia (the Virginia barrier
71 islands; VBI).

72 STUDY AREA

73 The southern 100 km of the U.S. Delmarva Peninsula is bounded on its eastern
74 side by a chain of largely undeveloped mixed-energy barrier islands. Our study area
75 included the nine barrier systems from Assawoman to Smith islands (Fig. 1). These
76 islands are 3–12 km long, 100–1000 m wide, are located 2.0–13.5 km offshore, and are
77 backed by varying proportions of salt marshes, tidal flats, and shallow (1–2 m) open-
78 water bays. The VBI are sub-divided into three geomorphic groups (Fig. 1): (1) a
79 northern group characterized by parallel retreat (landward migration); (2) a central
80 rotational group characterized by classic drumstick morphology; and (3) a southern group
81 undergoing non-parallel beach retreat (Leatherman et al., 1982; Rice and Leatherman,
82 1983). Tropical and extratropical storms and their associated wave regimes drive a net
83 southerly longshore transport along the ocean side of this system.

84 The VBI have experienced some of the highest rates of RSLR along the US
85 Atlantic Coast: at Kiptopeke, VA (see location, Fig. 1) rates over the past 50 years were
86 *ca.* 3.7 mm yr⁻¹ (Boon and Mitchell, 2015. The VBI are allowed to erode and migrate
87 without human interference, making them the largest natural barrier system along the
88 U.S. Atlantic Coast, and an excellent location to test how barrier islands respond to
89 accelerated RSLR in the absence of development.

90 METHODS

91 Historical shoreline positions (mean high water) along the VBI were digitized for
92 1851–1997 by Himmelstoss et al. (2010). We delineated an additional set of shoreline
93 positions from 2010 LiDAR (USGS, 2011) following procedures of Himmelstoss et al.
94 (2010). We then calculated shoreline change rates for this combined dataset along
95 transects spaced at 50 m intervals as the slope of linear regressions between shoreline
96 date and position using the Digital Shoreline Analysis System (DSAS) plugin for ESRI
97 ArcGIS (Thieler et al., 2009). We computed both long-term (1851/2–2010) and short-
98 term (1851/2–1910/1; 1980–2010) island-averaged rates. Errors in shoreline-change rates
99 were determined after Hapke et al. (2011); see data repository for details.

100 Historical backbarrier marsh and water areas were derived from NOS T-sheets
101 (Table DR1) by digitizing the marsh-water boundary at map scale (1:20,000).
102 Classification of 2009 aerial imagery of the VBI (VGIN, 2009) using unsupervised
103 classification in ArcGIS was manually down-sampled to the 1:20,000 resolution of
104 historical maps, thereby excluding narrow interior marsh creeks, as in the T-sheets.
105 Because the T-sheets were mapped at different years (Table DR1), we normalized all
106 historical marsh areas to the mean map year (1870) by assuming marsh area changed at a
107 constant rate from the mapping year to 2009.

108 The VBI were sub-divided into individual island systems based on hydrodynamic
109 properties. “Baysheds” — the areas drained and filled by a given inlet during ebbing and
110 flooding tides — were delineated using bathymetry and topography, creating a marine
111 equivalent of watersheds. Each island is hydrologically associated with the two baysheds
112 (Figure DR1a), corresponding to its two adjacent inlets; thus, the “barriershed” and its
113 associated tidal prism for a given island is herein defined as the sum of those two

114 associated baysheds. TP* (a proxy for tidal prism based on local tidal range [1.4 m] and
115 relative area of backbarrier open-water and intertidal land; detailed calculation in Data
116 Repository), marsh extent, and changes therein were calculated for each barriershed and
117 compared to shoreline change rates.

118 RESULTS

119 Long-term (1850/1–2010) island-averaged shoreline-retreat rates are 1.2–6.2 m
120 yr^{-1} ; the average system-wide retreat rate was 5.1 m yr^{-1} (Table DR2; Fig. 1), consistent
121 with system-wide 20th century estimates of *ca.* 5 m yr^{-1} (Leatherman et al., 1982). Short-
122 term (1980–2010) retreat rates were generally higher, reaching nearly 20 m yr^{-1} . System-
123 wide short-term shoreline retreat was 7.0 m yr^{-1} , which is more than 25x higher than the
124 average retreat rate for the Mid-Atlantic and New England coasts (Hapke et al., 2013).
125 Previous studies (e.g., Richardson and McBride, 2007, 2011; Nebel et al., 2012) have
126 documented similar shoreline change rates for individual VBI, including the observed
127 recent acceleration (see data repository and Table DR3 for complete discussion).

128 Modern barriershed TP* values range from $35 \times 10^6 \text{ m}^3$ to $362 \times 10^6 \text{ m}^3$ (Table
129 DR4, DR5). Net change in TP* (1870–2009) ranges from a loss of $16.6 \times 10^6 \text{ m}^3$
130 (-19.5%) to a gain of $19.5 \times 10^6 \text{ m}^3$ ($+4.4\%$) (Fig. 2). Total change in TP* within the
131 study area was a loss of $< 0.1\% \pm 4\%$. Individual baysheds experienced changes in TP*
132 ranging from +11% where backbarrier marsh loss was greatest, to -31% in regions
133 experiencing a decrease in backbarrier area due to island rollover (Figure DR1). Changes
134 in marsh area were calculated as a net loss between 1870 and 2009 of 62.9 km^2 , or 19.3%
135 of the 1870 marsh extent, a rate of $0.45 \text{ km}^2 \text{ yr}^{-1}$ ($0.1\% \text{ yr}^{-1}$). This is lower than more
136 recent rates observed in subsections of the VBI (Sepanik and McBride, 2015 and

137 references therein), likely reflecting a late 20th century acceleration in marsh loss (see
138 data repository and Table DR6 for complete discussion). As first recognized for the VBI
139 by Knowlton (1971), we observe that burial resulting from island migration (calculated as
140 the area of historical marsh located seaward of the 2009 island-backbarrier shoreline) is
141 responsible for the majority (32.3 km²; 51.4%) of marsh loss across the VBI (Figs. 2a,
142 DR1; Table DR4). Although our methods cannot capture conversion of high marsh to low
143 marsh, we find no evidence of interior marsh drowning. Backbarrier marsh loss (30.6
144 km²) is largely along the edges of open-water bays (Fig. 1d): such locations have larger
145 fetch, thereby allowing for the development of larger waves and enhanced marsh-edge
146 erosion (Mariotti and Fagherazzi, 2013; McLoughlin et al., 2015).

147 **DISCUSSION**

148 Barrier island / backbarrier ecogeomorphic couplings have been proposed as a
149 dominant driver of barrier system change in response to RSLR. For example, exploratory
150 numerical models of landscape-scale ecomorphodynamic couplings (e.g., Lorenzo-
151 Trueba and Ashton, 2014; Walters et al., 2014; Brenner et al., 2015) point to mutually
152 beneficial coupling between marshes and barrier islands. Similarly, the conceptual
153 “runaway transgression” model (FitzGerald et al., 2008) predicts that submergence of
154 backbarrier marshes under conditions of rapid RSLR will lead to an increase in
155 backbarrier open-water area and tidal prism, causing an increase in the number and size
156 of tidal inlets, sand sequestration in ebb-tidal deltas, and attendant accelerated beach
157 erosion and barrier island narrowing.

158 Our findings are in direct contrast to this conceptual framework: we find strong
159 negative relationships between shoreline retreat rate and both modern TP* (2009) and

160 change in TP* (1870–2009) in the VBI (Fig. 3), rather than the positive relationships
161 anticipated from the runaway transgression model. This implies that islands fronting
162 barriersheds with a larger and/or increasing tidal prism have historically had a slower
163 retreat rate than those with a smaller and/or diminishing tidal prism. Shoreline retreat
164 rates instead likely reflect drivers not directly related to barrier-marsh
165 ecomorphodynamic feedbacks. For example, along the northern VBI, relatively high rates
166 of island migration have been attributed to updrift sand trapping at Fishing Point, as
167 Assateague Island progrades southward into deeper water (Leatherman et al., 1982);
168 southerly extension of the resulting erosional ‘Chincoteague Bight’ may have caused the
169 recent acceleration in shoreline retreat on Cedar and Parramore islands (Richardson and
170 McBride, 2007; Oertel et al., 2008; Nebel et al., 2012). Other factors influencing
171 variability in retreat rates may include geologic framework (Belknap and Kraft, 1985;
172 Moore et al., 2010), differential subsidence rates (Leatherman et al., 1982), paleo-
173 channels (Oertel et al., 2008), substrate and backbarrier sand/mud content and erodibility
174 (Brenner et al., 2015), inlet ebb-delta dynamics influencing longshore transport (Fenster
175 et al., 2016), and rates of storm-driven overwash (Lorenzo-Trueba and Ashton, 2014).

176 Regardless of the responsible mechanisms for shoreline change on any given
177 island, we find that, especially given our observed minimal upland marsh migration (Fig.
178 DR1), barrier island migration has driven a net loss of marsh and backbarrier area
179 through time. Although a clear lack of evidence exists that this shoreline retreat is in
180 direct response to changes in tidal prism at the scale of individual islands (Fig. 3), the
181 near-zero net change (d of <0.1%) in TP* for the VBI as a whole between 1870 and 2009
182 (Fig. 2b) suggests that the VBI may be responding to coastal change in a system-wide

183 (multi- inlet and island) manner. Unlike in the model of FitzGerald et al. (2008), which
184 initiates with stable, non-migratory barrier islands that remain stationary as the marshes
185 deteriorate and tidal prism increases, the VBI are sand-starved and have been
186 eroding/migrating throughout the period of study. Thus, they may represent barrier
187 systems already undergoing runaway transgression; in this case, the small net temporal
188 change in TP* for the island chain as a whole may reflect a dynamic equilibrium in which
189 gains in TP* due to backbarrier marsh loss across the system are balanced by losses in
190 TP* due to rapid landward migration of the overwash-dominated northern and southern
191 islands.

192 CONCLUSIONS

193 Along the VBI, we find that barrier-island retreat and the attendant narrowing of
194 backbarrier regions is the primary ecomorphodynamic coupling between barrier islands
195 and backbarrier environments. This coupling is also the leading driver of marsh loss in
196 the mixed-energy VBI, accounting for over half of a net reduction in marsh area of 19%
197 from 1870 to 2009. Such barrier-backbarrier interactions can be expected in similar
198 mixed-energy barrier systems (e.g., South Carolina, New Jersey, Germany, and
199 elsewhere), especially in cases where steep uplands prevent upland marsh migration from
200 balancing losses to landward barrier island migration. Moreover, we find that this
201 coupling is specific to those islands undergoing landward migration, and not simply
202 shoreline erosion. Once narrowing leads to the initiation of island migration, it appears
203 that this migration and associated marsh loss overwhelm the potential effects of interior
204 marsh loss on barrier island stability. Artificial stabilization of barrier islands may
205 provide short-term resistance to the impacts of migration; however, it decreases system

206 resilience to RSLR in the long term (Rogers et al., 2015). Thus, regardless of the ability
207 of vertical marsh accretion to keep pace with RSLR, large-scale marsh loss may be
208 inevitable as barrier systems worldwide equilibrate to accelerated RSLR.

209

210 **ACKNOWLEDGMENTS**

211 We thank R. McBride, J. Lorenzo Trueba, L. Moore, D. Walters, and two
212 anonymous reviewers for comments and conversations which greatly improved this
213 manuscript. This work was supported financially by NSF LTER (1237733) and Coastal
214 SEES (1426981 and 1325430) programs. This is contribution #xxx of the Virginia
215 Institute of Marine Science.

216 **REFERENCES CITED**

217 Barbier, E.B., Hacker, S.D., Kennedy, C., Koch, E.W., Stier, A.C., and Silliman, B.R.,
218 2011, The value of estuarine and coastal ecosystem services: Ecological
219 Monographs, v. 81, p. 169–193, doi:10.1890/10-1510.1.

220 Belknap, D.F., and Kraft, J.C., 1985, Influence of antecedent geology on stratigraphic
221 preservation potential and evolution of Delaware's barrier systems: Marine Geology,
222 v. 63, p. 235–262, doi:10.1016/0025-3227(85)90085-4.

223 Bird, E.C.F., 1985, Coastline changes: A global review: New York, NY, John Wiley and
224 Sons, Inc., 219 p.

225 Boon, J.D., and Mitchell, M., 2015, Nonlinear change in sea level observed at North
226 American tide stations: Journal of Coastal Research, v. 31, p. 1295–1305,
227 doi:10.2112/JCOASTRES-D-15-00041.1.

228 Brenner, O.T., Moore, L.J., and Murray, A.B., 2015, The complex influences of back-
229 barrier deposition, substrate slope and underlying stratigraphy in barrier island
230 response to sea-level rise: Insights from the Virginia Barrier Islands, Mid-Atlantic
231 Bight, U.S.A: Geomorphology, v. 246, p. 334–350,
232 doi:10.1016/j.geomorph.2015.06.014.

233 Fenster, M.S., Dolan, R., and Smith, J.J., 2016, Grain-size distributions and coastal
234 morphodynamics along the southern Maryland and Virginia barrier islands:
235 Sedimentology, v. 63, p. 809–823, doi:10.1111/sed.12239.

236 FitzGerald, D.M., Fenster, M.S., Argow, B.A., and Buynevich, I.V., 2008, Coastal
237 impacts due to sea-level rise: Annual Review of Earth and Planetary Sciences, v. 36,
238 p. 601–647, doi:10.1146/annurev.earth.35.031306.140139.

239 Hapke, C.J., Himmelstoss, E.A., Kratzmann, M., List, J.H., and Thieler, E.R., 2011,
240 National assessment of shoreline change: historical shoreline change along the New
241 England and Mid-Atlantic Coasts: U.S. Geological Survey Open-File Report 2010–
242 1118, 57 p.

243 Hapke, C.J., Kratzmann, M.G., and Himmelstoss, E.A., 2013, Geomorphic and human
244 influence on large-scale coastal change: Geomorphology, v. 199, p. 160–170,
245 doi:10.1016/j.geomorph.2012.11.025.

246 Himmelstoss, E.A., Kratzmann, M., Hapke, C.J., Thieler, E.R., and List, J.H., 2010, The
247 national assessment of shoreline change: A GIS compilation of vector shorelines and
248 associated shoreline change data for the New England and Mid-Atlantic Coasts: U.S.
249 Geological Survey Open-File Report 2010–1119, <http://pubs.usgs.gov/of/2010/1119>.

250 Kirwan, M.L., and Megonigal, J.P., 2013, Tidal wetland stability in the face of human
251 impacts and sea-level rise: *Nature*, v. 504, p. 53–60, doi:10.1038/nature12856.

252 Kirwan, M.L., Temmerman, S., Skeehan, E.E., Guntenspergen, G.R., and Fagherazzi, S.,
253 2016, Overestimation of marsh vulnerability to sea level rise: *Nature Climate
254 Change*, v. 6, p. 253–260, doi:10.1038/nclimate2909.

255 Knowlton, S.M., 1971, Geomorphological history of tidal marshes, Eastern Shore,
256 Virginia, from 1852–1966 [M.S. Thesis]: University of Virginia, 46 p.

257 Leatherman, S.P., Rice, T.E., and Goldsmith, V., 1982, Virginia Barrier Island
258 configuration: A reappraisal: *Science*, v. 215, p. 285–287,
259 doi:10.1126/science.215.4530.285.

260 Lorenzo-Trueba, J., and Ashton, A.D., 2014, Rollover, drowning, and discontinuous
261 retreat: Distinct modes of barrier response to sea-level rise arising from a simple
262 morphodynamic model: *Journal of Geophysical Research: Earth Surface*, v. 119,
263 p. 779–801, doi:10.1002/2013JF002941.

264 Lorenzo-Trueba, J., and Mariotti, G., 2015, Chasing Boundaries and Cascade Effects in a
265 Coupled Barrier - Marshes - Lagoon System, *in* Wang, P., Rosati, J.D., and Cheng,
266 J., eds., *Proceedings of the Coastal Sediments*: San Diego, USA, 11 p.,
267 doi:10.1142/9789814689977_0010.

268 Mariotti, G., and Fagherazzi, S., 2013, Critical width of tidal flats triggers marsh collapse
269 in the absence of sea-level rise: *Proceedings of the National Academy of Sciences of
270 the United States of America*, v. 110, p. 5353–5356, doi:10.1073/pnas.1219600110.

271 McLoughlin, S.M., Wiberg, P.L., Safak, I., and McGlathery, K.J., 2014, Rates and
272 forcing of marsh edge erosion in a shallow coastal bay: *Estuaries and Coasts*, v. 38,
273 p. 620–638, doi: 10.1007/s12237-014-9841-2.

274 Moore, L.J., List, J.H., Williams, S.J., and Stolper, D., 2010, Complexities in barrier
275 island response to sea level rise: Insights from numerical model experiments, North
276 Carolina Outer Banks: *Journal of Geophysical Research*, v. 115, p. F03004,
277 doi:10.1029/2009JF001299.

278 Nebel, S.H., Trembanis, A.C., and Barber, D.C., 2012, Shoreline analysis and barrier
279 island dynamics: Decadal scale patterns from Cedar Island, Virginia: *Journal of
280 Coastal Research*, v. 28, p. 332–341, doi:10.2112/JCOASTRES-D-10-00144.1.

281 Oertel, G.F., Allen, T.R., and Foyle, A.M., 2008, The influence of drainage hierarchy on
282 pathways of barrier retreat: An example from Chincoteague Bight, Virginia, U.S.A:
283 *Southeastern Geology*, v. 45, p. 179–201.

284 Rice, T.E., and Leatherman, S.P., 1983, Barrier island dynamics: The Eastern Shore of
285 Virginia: *Southeastern Geology*, v. 24, p. 125–137.

286 Richardson, T.M., and McBride, R.A., 2007, Historical shoreline changes and
287 morphodynamics of Parramore Island, Virginia (1852–2006), *in* Kraus, N.C., and
288 Rosati, J.D., eds., *Proceedings, Sixth International Symposium on Coastal
289 Engineering and Science of Coastal Sediment Processes*, American Society of Civil
290 Engineers, p. 364–377.

291 Richardson, T.M., and McBride, R.A., 2011, Historical shoreline changes and
292 morphodynamics of Cedar Island, Virginia, USA: 1852–2010, *in* Wang, P., Rosati,
293 J.D., and Roberts, T.M., eds., *Proceedings, Seventh International Symposium on*

294 Coastal Engineering and Science of Coastal Sediment Processes, World Scientific, p.
295 1285–1299.

296 Rodriguez, A.B., Fegley, S.R., Ridge, J.T., VanDusen, B.M., and Anderson, N., 2013,
297 Contribution of aeolian sand to backbarrier marsh sedimentation: Estuarine, Coastal
298 and Shelf Science, v. 117, p. 248–259, doi:10.1016/j.ecss.2012.12.001.

299 Rogers, L.J., Moore, L.J., Goldstein, E.B., Hein, C.J., Lorenzo-Trueba, J., and Ashton,
300 A.D., 2015, Anthropogenic controls on overwash deposition: Evidence and
301 consequences: Journal of Geophysical Research: Earth Surface, v. 120, p. 2609–
302 2624, doi:10.1002/2014JF003270.

303 Sepanik, J.M., and McBride, R.A., 2015, Salt-marsh loss in a barrier-island system:
304 Parramore and Cedar Islands, Virginia, *in* McBride, et al., Holocene barrier-island
305 geology and morphodynamics of the Maryland and Virginia open-ocean coasts:
306 Fenwick, Assateague, Chincoteague, Wallops, Cedar, and Parramore Islands, *in*
307 Brezinski, D.K., Halka, J.P., and Ortt, R.A., Jr., eds., Tripping from the Fall Line:
308 Field Excursions for the GSA Annual Meeting, Baltimore, 2015: Geological Society
309 of America Field Guide 40, p. 392–401, doi:10.1130/2015.0040(10).

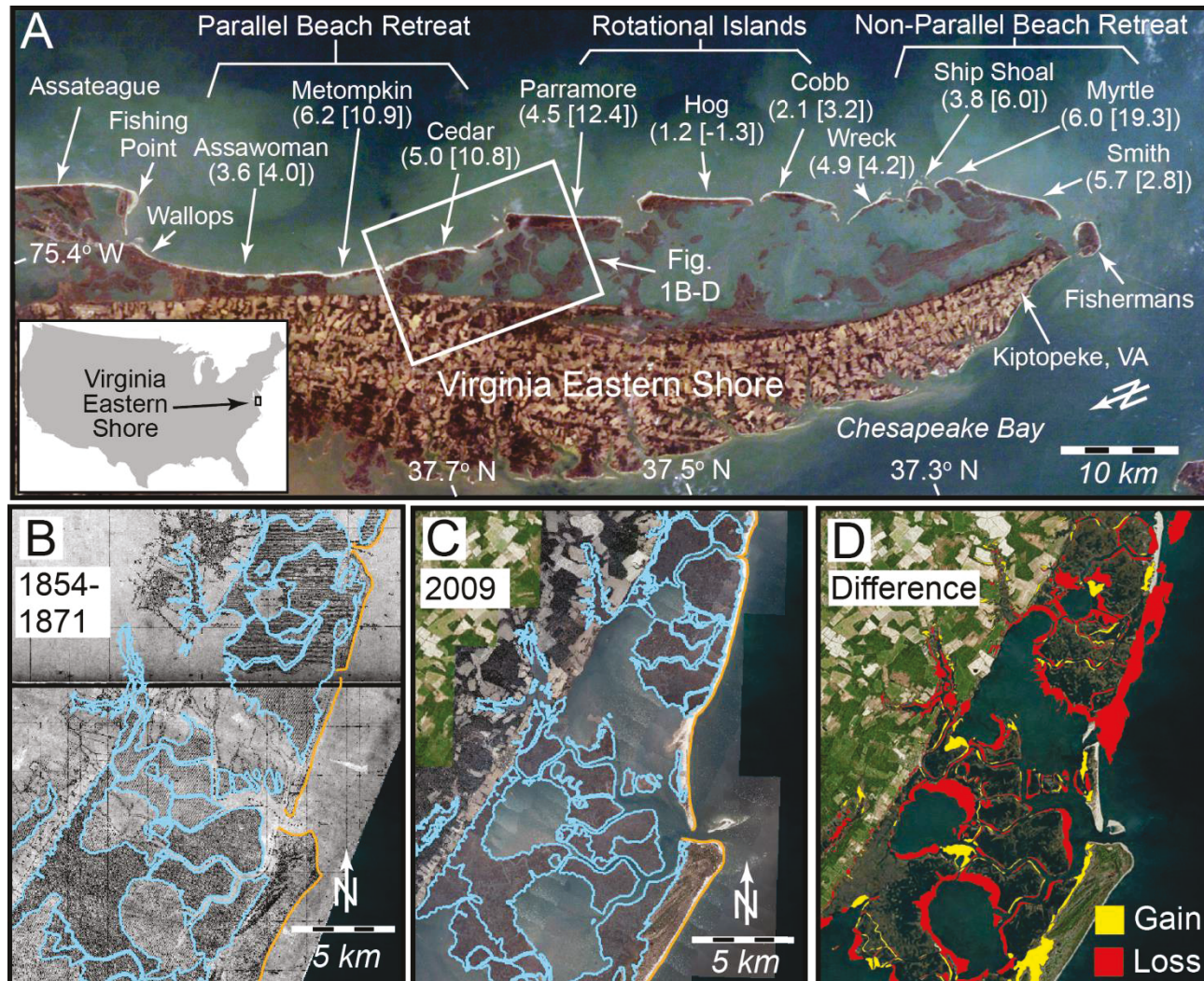
310 Stutz, M.L., and Pilkey, O.H., 2011, Open-ocean barrier islands: Global influence of
311 climatic, oceanographic, and depositional settings: Journal of Coastal Research,
312 v. 27, p. 207–222, doi:10.2112/09-1190.1.

313 Thieler, E.R., Himmelstoss, E.A., Zichichi, J.L., and Ergul, A., 2009, Digital Shoreline
314 Analysis System (DSAS) version 4.0—An ArcGIS extension for calculating
315 shoreline change: U.S. Geological Survey Open-file Report 2008–1278.

Publisher: GSA
Journal: GEOL: Geology
DOI:10.1130/G38459.1

316 U.S. Geological Survey (USGS), 2011, Eastern Shore Virginia (ESVA) LiDAR Project:
317 <http://virginalidar.com/index-3.html> (accessed August 2015).
318 Vellinga, P., and Leatherman, S.P., 1989, Sea level rise, consequences and policies:
319 Climatic Change, v. 15, p. 175–189, doi:10.1007/BF00138851.
320 Virginia Geographic Information Network (VGIN), 2009, Virginia Base Mapping
321 Project: <http://gismaps.vita.virginia.gov/arcgis/services> (accessed Aug. 2014).
322 Walters, D., Moore, L.J., Vinent, O.D., Fagherazzi, S., and Mariotti, G., 2014,
323 Interactions between barrier islands and backbarrier marshes affect island system
324 response to sea level rise: Insights form a coupled model: Journal of Geophysical
325 Research: Earth Science, v. 119, p. 2013–2031, doi:10.1002/2014JF003091.
326

327 FIGURES



329 Figure 1. A) Virginia barrier islands. Numbers in parentheses are island-averaged long-term (1851/2–2010) and short-term (1980–
330 2010; in brackets) shoreline retreat rates in m yr^{-1} from linear regressions of shoreline position and date. Satellite image is modified
331 from NASA image ISS006-E-13525. B)-D) Marsh extent (blue lines) behind Cedar and northern Parramore islands in the mid- to late-
332 1800s (B) and 2009 (C), and the gain/loss in marsh area between in the intervening >140 years (D). 1854 (northern Cedar) and 1871
333 (southern Cedar and northern Parramore) data are derived from NOAA T-sheets T-01200 and T-00512, respectively. Modern data are
334 derived from digital classification of 2009 aerial orthoimagery.

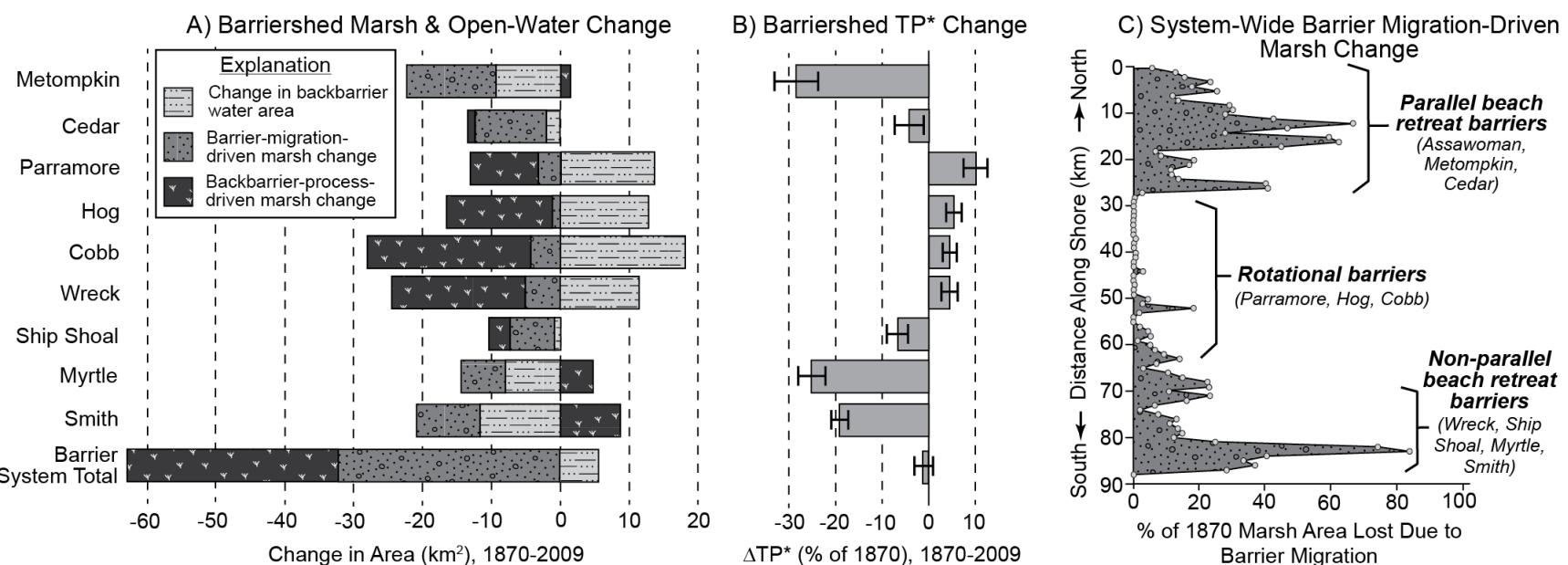
335

336

337

338

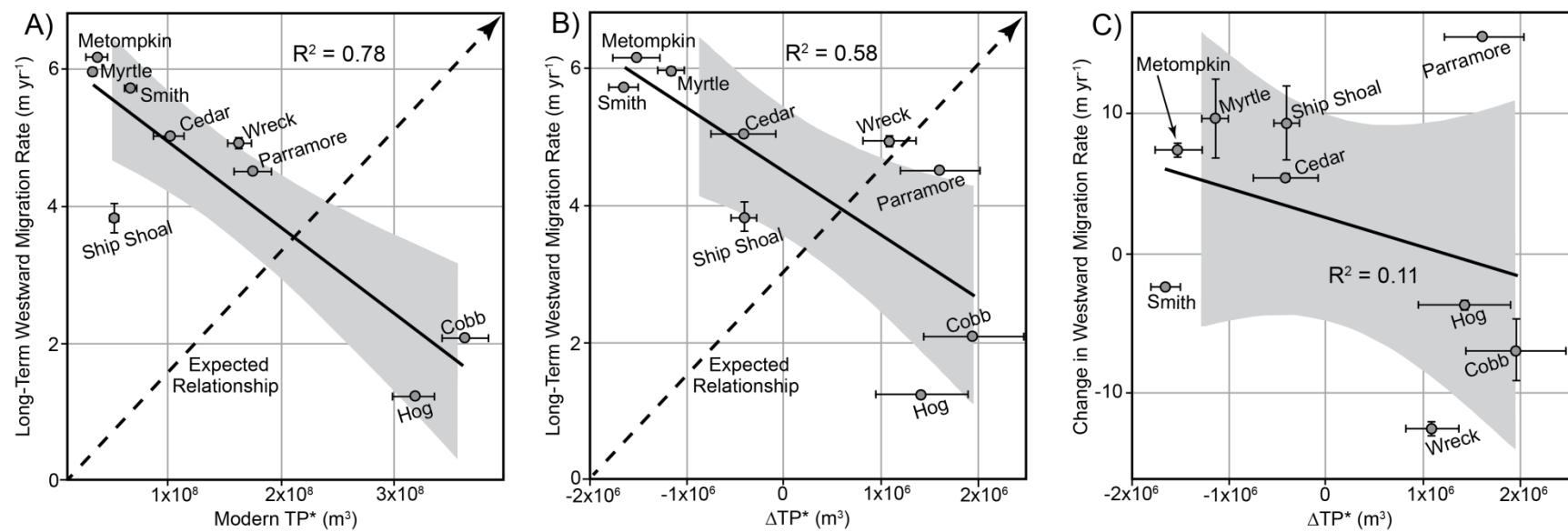
339



340

341 Figure 2. Marsh and tidal prism change along the Virginia barrier islands, 1870–2009. A) Change in open-water area and marsh area
 342 due to barrier migration and backbarrier processes (dominantly edge erosion). Barrier-migration-driven marsh loss is that marsh which
 343 has been buried by westward-migrating islands. B) Change in tidal prism (as denoted by TP*) along the Virginia barrier islands. C)
 344 Marsh loss (% of 1870) due to barrier migration within 1-km wide (alongshore) bins.

345



346

347 Figure 3. Comparisons between barrier retreat rates and backbarrier properties: A)-B) Long-term (1851/2–2010) retreat rates versus
 348 (A) modern TP* and (B) change in TP* (1870–2009). C) Change in retreat rate (difference between rate for 1851/2–1910/1 and 1980–
 349 2010) versus change in TP* (1870–2009). Solid lines: linear regression fits; Gray windows: standard error. Expected relationships are
 350 illustrated as a dashed line in each plot, with slope and intercept approximated for illustrative purposes. Errors are within data symbols
 351 where bars not shown.